



Chemically Bonded Porogens in Methylsilsesquioxane

I. Structure and Bonding

Agnes M. Padovani,^{a,*} Larry Rhodes,^b Sue Ann Bidstrup Allen,^a
and Paul A. Kohl^{a,*,*,z}

^aSchool of Chemical Engineering, Georgia Institute of Technology, Atlanta, Georgia 30332-0100, USA

^bPromerus LLC, Brecksville, Ohio 44141, USA

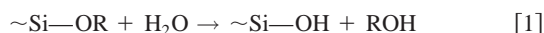
Porous methylsilsesquioxane (MSQ, CH₃SiO_{1.5}) films were created by making polymer blends with trimethoxysilyl norbornene (TMSNB) and triethoxysilyl norbornene (TESNB), where the polymer served as a sacrificial place-holder. Upon exposure to elevated temperatures, the polymers decomposed within the MSQ matrix to form nanosize voids in the films. Different pore microstructures were observed by transmission electron microscopy and atomic force microscopy, depending on the functional groups on the polymeric sacrificial material used. The differences in microstructure have been correlated to variations in the chemical reactivity between the sacrificial polymer and the MSQ matrix. Solid-state ²⁹Si and ¹³C nuclear magnetic resonance, and Fourier transform infrared spectroscopy have been used to study the chemical structure of the TMSNB and TESNB:MSQ mixtures. Indications of a chemical bond between the TMSNB and the MSQ have been found in these mixtures; however, the same results were not observed for the TESNB system. The addition of an acid catalyst to the TESNB was found to induce a reaction between the TESNB sacrificial polymer and the MSQ. The percent weight loss of the MSQ and its mixtures (with TMSNB and TESNB) were used to evaluate the polymer residue.

© 2002 The Electrochemical Society. [DOI: 10.1149/1.1515281] All rights reserved.

Manuscript received March 11, 2002. Available electronically October 16, 2002.

The use of trimethoxysilyl norbornene (TMSNB) and triethoxysilyl norbornene (TESNB) polymers as sacrificial place-holders for the development of porous, low dielectric constant methylsilsesquioxane (MSQ) films has been previously reported.¹ After spin-coating the silsesquioxane-norbornene mixture into a thin film, heating to 425°C decomposes the TMSNB and TESNB polymers within the MSQ films. The volatile decomposition products permeate through the silsesquioxane matrix creating a porous MSQ structure. The introduction of porosity lowers the dielectric constant of the MSQ films, which is necessary to be suitable for use as interlevel dielectrics for integrated circuits.² However, the successful application of porous materials has been limited by the ability to control the pore microstructure because pore sizes on the order of 10 to 20% (or less) of the smallest feature size would be acceptable for use in microelectronic devices.³ In light of these requirements, this work has focused on a method for the creation of porous films that involves chemically bonding the sacrificial material to the MSQ matrix, in an effort to control the resulting porosity.

MSQ resins require a high-temperature cure to increase the molecular weight and develop the ladder-like structure into a three-dimensional, insoluble, and mechanically stable network.⁴ In solution, the silsesquioxane contains terminal silanol groups (Si—OH) that undergo a condensation reaction upon heating to high temperature.⁵ The reaction creates Si—O—Si bonds between the MSQ oligomers with water as the by-product. The goal of chemically bonding the sacrificial polymer to the MSQ oligomers is to mitigate the problems associated with phase separation of the sacrificial material, thus controlling the resulting porosity microstructure (pore size and distribution), especially at high polymer loading. For this purpose, trialkoxysilyl moieties (TMS and TES) were chosen as pendant groups in the polynorbornene sacrificial material. The alkoxyisilyl groups can undergo a condensation reaction, which can be with another alkoxyisilyl group or with the MSQ oligomer (intra- or intermolecular). The hydrolysis and condensation reactions of alkoxyisilyl groups (Si—OR) are characteristic of sol-gel processing,⁶ as shown in Eq. 1 to 3



As can be seen from Eq. 1 and 2, low molecular weight alcohols can also be produced (methanol or ethanol in the case of TMS or TES, respectively) in addition to the water from the condensation of the silanol groups.

In this work, the chemical functionality and bonding of the porogen material to MSQ was studied. The chemical structure and the effect of MSQ-porogen bonding on the porosity microstructure and other film properties were evaluated.

Experimental

Honeywell 418 MSQ (Santa Clara, CA) was used as the matrix material. Trimethoxysilyl norbornene (TMSNB; Mw = 57,000) and triethoxysilyl norbornene (TESNB; Mw = 58,000) polymers (Promerus, Brecksville, OH) were used as the sacrificial materials. Homopolymers with pendant trialkoxysilyl groups were chosen so as to maximize the number of reactive sites for bonding with the MSQ matrix. Solutions of the sacrificial polymers were made in methyl isobutyl ketone (MIBK) and were then combined with the MSQ solution (also in MIBK) to the weight ratios specified in the text (solvent not included in the ratio).

To investigate alternative ways of promoting a chemical reaction between the sacrificial polymer and the MSQ matrix, the effect of an added acid that would serve as a catalyst in the hydrolysis and condensation reactions was studied for some of the TESNB:MSQ mixtures. The basic experiment consisted of adding a photoacid generator system (in which the acid forms upon exposure to UV radiation) into the mixture, or by direct addition of HCl to the TESNB:MSQ blend. In the case of the photoacid generator, the photoactive ingredients were dissolved in MIBK prior to mixing at 10 wt % concentration with the TESNB polymer. The samples were exposed to a 1000 mJ/cm² UV radiation dose before curing.

For the solid-state nuclear magnetic resonance (NMR) experiments, the polymer/MSQ solutions were poured into ceramic crucibles and heated to 250°C for 30 min or 350°C for 1 h in a nitrogen-purged furnace. The solutions were spun-cast onto KBr crystals for the Fourier transform infrared (FTIR) spectroscopy studies. Spectra were collected after curing at different temperatures. After spin-coating, the KBr crystals were baked in an oven at 180°C for 10 min, followed by a furnace cure that consisted of one or all of the following temperature cycles: 250°C for 30 min, 350°C for 30 min, and/or 425°C for 1.5 h. The final cure temperature of 425°C

* Electrochemical Society Student Member.

** Electrochemical Society Active Member.

^z E-mail: paul.kohl@che.gatech.edu

was necessary to decompose the sacrificial material and form the porous films. The decomposition products permeated through the MSQ matrix creating voids. In the case of thermogravimetric studies, the solvent was eliminated from the solutions prior to loading the samples into the chamber in order to avoid preliminary weight loss from evaporation. Transmission electron microscopy (TEM) was used to evaluate the porosity microstructure after decomposition of the sacrificial materials. The resulting pore sizes were analyzed from ultrathin cross sections prepared by focused ion beam etching. The surface topography of the porous films was measured using atomic force microscopy (AFM). The AFM images were recorded with a Nanoscope IIIa from Digital Instruments, Inc. Microfabricated silicon cantilevers were used in the tapping mode to avoid deformation and indentation of the sample surface by the tip.

Solid-state ^{29}Si and ^{13}C NMR experiments were performed with a Bruker DSX 400 spectrometer operating at 399.84 MHz (^1H resonance frequency). To improve the resolution in the solid-state (reduce line broadening), the samples were spun at 10 kHz in zirconia rotors at the magic angle (54.7°). Cross-polarization magic-angle spinning (CP-MAS) experiments were performed in all cases due to the relatively long relaxation times of the nuclei. Experiments with pure MSQ showed that the average T_1 (spin-lattice relaxation times) for the silicon nuclei in MSQ were 34 and 34.6 s for the T^2 and T^3 species, respectively. The cross-polarization technique was used, along with MAS and dipolar decoupling, to reduce the experiment time, as well as to improve the signal-to-noise ratio and the resolution of the spectra. The shortened experimental times are a result of the interaction of the proton nuclei (^1H) with the fields of the ^{29}Si or ^{13}C nuclei (in a cross-polarization pulse sequence) that causes faster relaxation, and thus reduces the delay time between pulses (typically four to five times T_1).⁷ Dipolar decoupling consists of irradiating the sample at proton frequencies during the acquisition of the spectra to remove dipolar splitting.⁸ ^{29}Si nuclear magnetic resonance (NMR) spectra were collected at 79.44 MHz, and the chemical shifts were calibrated with the sodium salt of 2,2-dimethyl-2-silapentane-5-sulfonic acid (DSS). The largest peak of the DSS spectrum was referenced with respect to tetramethylsilane (TMS) (9.74 ppm from TMS). Typical measurement conditions were as follows: ^1H 90° pulse width, 4.85 μs ; repetition delay, 10 s; number of scans, 1024; cross-polarization contact time, 3 ms (predetermined to yield the highest intensity for the MSQ peaks). ^{13}C NMR spectra were obtained at 100.55 MHz using adamantane as the calibration standard for the chemical shifts (37.8 ppm from TMS). The measurement conditions for these experiments were as follows: ^1H 90° pulse width, 3.95 μs ; repetition delay, 4 s; number of scans, 1024; CP contact time, 0.1 or 1 ms.

FTIR spectra were collected in transmission mode using a Nicolet Magna-IR 560 spectrometer. All spectra were recorded at a resolution of 4 cm^{-1} and averaged over 512 scans. The background spectrum of each KBr crystal was measured prior to depositing the films.

The thermogravimetric analysis (TGA) was performed using a Seiko TG/DTA 320 analyzer. The samples were purged with nitrogen during the temperature cycles to remove the oxygen from the chamber. The temperature profile used for these samples was to ramp to 425°C at $2^\circ\text{C}/\text{min}$, followed by holding at 425°C for 1.5 h. This profile was chosen to simulate the typical cure process used to create the porous films. The weight loss of the samples was monitored as a function of temperature and time.

Results

TEM was used to study the pore microstructure of the TMSNB:MSQ samples. Figure 1 shows a cross section of a 30 wt % TMSNB, 70 wt % MSQ (30:70 wt % TMSNB:MSQ) film after decomposition of the sacrificial polymer (TMSNB). The lighter (less electron dense) regions in the image correspond to the porosity. The results show pores of nearly spherical geometry with diameters of ~ 3 to 10 nm. TEM analysis of films formed with higher TMSNB

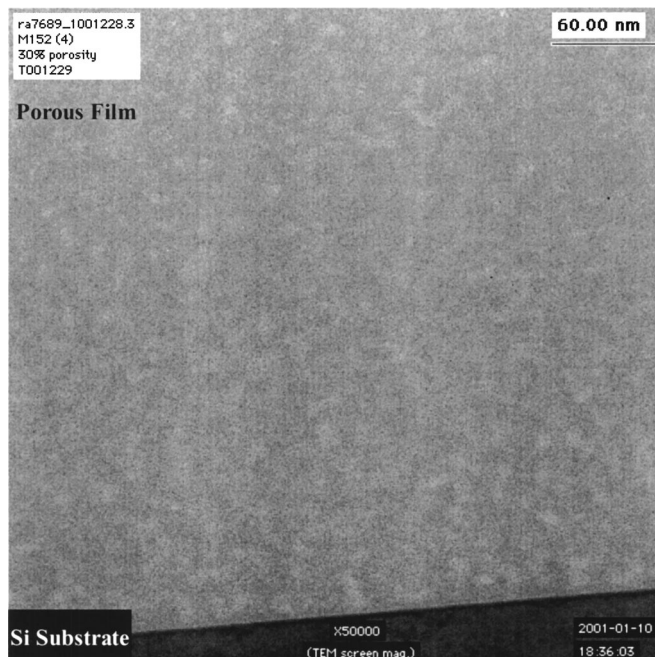


Figure 1. TEM cross section of a 30:70 wt % TMSNB:MSQ film after decomposition of the sacrificial material.

concentrations showed that the pore sizes were the same regardless of the amount of sacrificial material added to the films, at least in the range 10 to 40 wt % TMSNB. This shows that the polymer does not phase segregate from the MSQ matrix. Phase separation is inhibited by chemically bonding the polymer to the MSQ backbone. In studies elsewhere,^{9,10} poly(ϵ -caprolactone) has been shown to phase segregate from silsesquioxane backbones within this concentration range.

Transmission electron micrographs of films created using the TESNB sacrificial polymer showed significant differences from the TMSNB results. In the case of TESNB, no nanometer-scale porosity was observed within the bulk of the MSQ films regardless of the concentration of the sacrificial polymer used to prepare the films (0-30 wt % TESNB). Investigation of the TESNB samples showed the development of large cavities on the surface of the films after decomposition of the sacrificial polymer. An AFM surface topography image of a 10:90 wt % TESNB:MSQ film after decomposition of the sacrificial material is shown in Fig. 2. The results show surface cavities with an average diameter of 300 nm and depth of ~ 50 nm. Higher loading of TESNB in the films resulted in higher concentration of surface pores.

The large surface pores are hypothesized to be the result of phase separation of the TESNB from the MSQ matrix, which did not occur with the TMSNB sacrificial system. The higher reactivity of TMSNB for chemical bonding to MSQ is assumed responsible for it retaining its position within the MSQ host matrix. To test this hypothesis, a series of experiments were performed to increase the reactivity of the TESNB with MSQ. The hydrolysis and condensation reaction between TESNB and MSQ can be acid catalyzed.¹¹ Therefore, Rhodorsil photoacid generator (PAG; tetrakis(pentafluorophenyl) boratede 4-methylphenyl [4-(1-methylethyl)phenyl] iodonium) was added to a 10:90 wt % TESNB:MSQ mixture to catalyze the reactions. The results showed that the surface rms (root mean square) roughness for the 10:90 wt % TESNB:MSQ film after cure at 425°C for 1.5 h reduced from 28 nm for the film without acid, to 5 nm for the film with PAG. However, additional TEM investigation is required to determine if nanometer-size porosity developed within the bulk of the film.

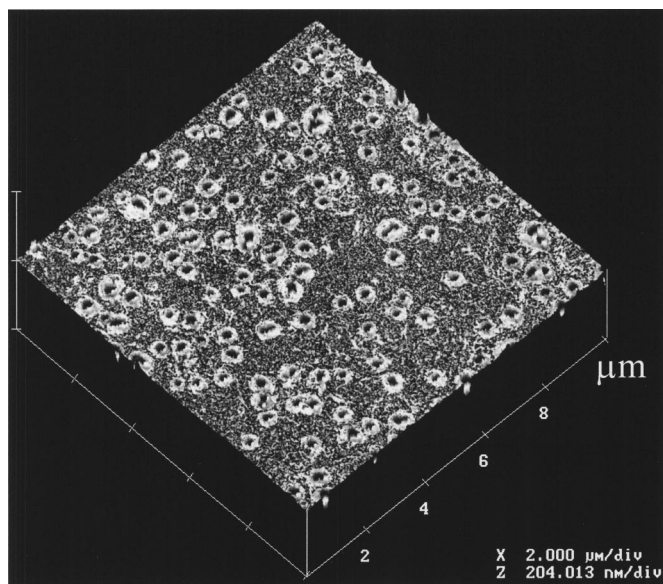


Figure 2. AFM image showing surface topography of a 10:90 wt % TESNB:MSQ film after decomposition of the sacrificial polymer.

A similar experiment conducted with a 75:25 (mol %) copolymer ($M_w = 63,000$) of TESNB with butyl norbornene (BuNB) as the sacrificial material instead of the TESNB homopolymer showed a comparable improvement with the introduction of a PAG to the system. In this case, the acid addition was considered necessary to compensate for the lower concentration of reactive side groups in the sacrificial polymer: 75 mol % TESNB in the copolymer as opposed to 100 mol % in the TESNB homopolymer. For this test, 10 wt % of the PAG was added to a 10:90 wt % mixture of the TESNB/BuNB copolymer with MSQ. The pore microstructure was evaluated with TEM after heat-treatment at 425°C for 1.5 h. The results showed that the pores were reduced from a range of 200 to 300 nm in diameter (for a film without the PAG) to about 50 nm with the addition of the PAG into the sacrificial polymer-MSQ mixture. Therefore, this indicates that when the concentration of reactive side groups was reduced, the acid-catalyzed reaction could mitigate some of the effects of phase separation.

Solid-State ^{29}Si NMR.—High-resolution solid-state ^{29}Si NMR experiments were conducted to investigate the chemical structure of the porogen-MSQ polymer blends as a function of cure temperature. Figure 3 shows the ^{29}Si NMR spectra for MSQ after cure at (a) 250°C for 30 min, and (b) 350°C for 1 h. The spectra show two types of silicon atoms at -58 and -65 ppm (upfield from TMS⁷), which correspond to T^2 and T^3 species, respectively. The notation refers to standard nomenclature for silicate compounds, which differentiates between fully densified silica structures (SiO_2 , denoted as Q) and silsesquioxanes (denoted as T species). In the case of the silsesquioxanes, each silicon atom is bonded to an average of 1.5 oxygen atoms, and the remaining silicon bond is nonbridging typically to an H or an alkyl group (CH_3 in the case of MSQ). The number following the species type refers to the number of O—Si groups that are bonded to each silicon atom.¹² Thus, the T^2 species in the MSQ spectrum refers to silicon atoms with hydroxyl group terminations [$\text{CH}_3\text{Si}\cdot(\text{OSi})_2\text{OH}$], and the T^3 refer to the silicon nuclei within the bulk of the network having three —O—Si bonds and one CH_3 group [$\text{CH}_3\text{Si}\cdot(\text{OSi})_3$].^{11,13,14} These structural differences have been labeled in the MSQ molecule shown in Fig. 3, and the corresponding peaks in the spectra have also been identified. Integration of the peaks shows that after the 250°C cure, 29% of the silicon atoms in MSQ are of the T^2 type and 71% are T^3 species. However, after curing at 350°C for 1 h, the concentration of T^2

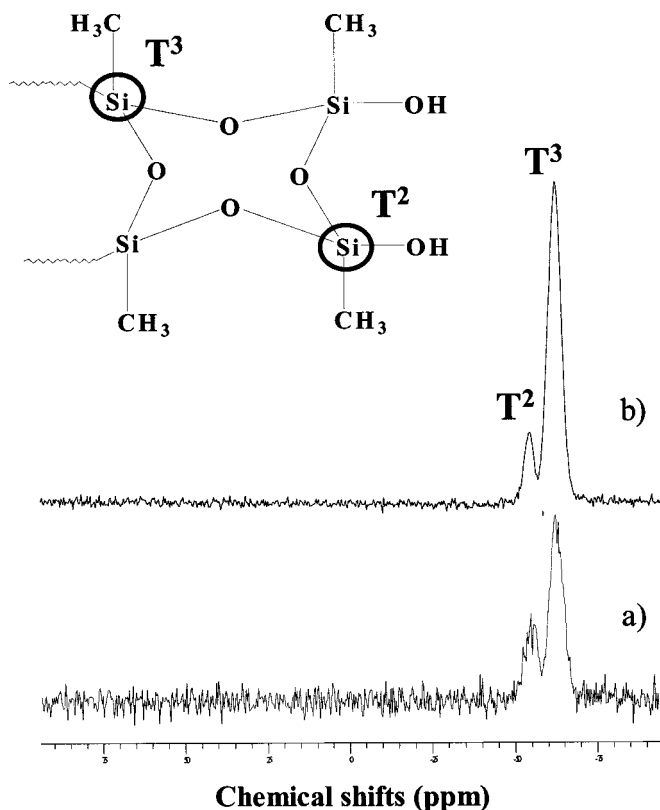


Figure 3. Molecular structure of MSQ and ^{29}Si NMR spectra after cure at (a) 250°C for 30 min and (b) 350°C for 1 h.

species is only 16% with the remainder being T^3 species. The reduction in the concentration of T^2 species between 250 and 350°C is due to the condensation reaction of the —OH groups forming Si—O—Si units in MSQ.

The ^{29}Si NMR spectrum for TMSNB after curing at 350°C for 1 h is shown in Fig. 4. The spectrum consists of a major peak at -44 ppm, and two shoulders at -40 and -50 ppm. Following the notation described previously, the peak at -44 ppm in TMSNB corresponds to T^1 silicon atoms [$\text{NB-Si}\cdot(\text{OSi})(\text{OCH}_3)_2$], and the peaks at -40 and -50 ppm, to T^0 [$\text{NB-Si}\cdot(\text{OCH}_3)_3$] and T^2 [$\text{NB-Si}\cdot(\text{OSi})_2\text{OCH}_3$], respectively.^{11,13} T^0 species correspond to TMSNB molecules where none of the methoxy groups has reacted to form Si—O—Si linkages. A very small T^0 peak was observed after the temperature cycles at 250 and 350°C . Deconvolution techniques were used to resolve the three peaks, and the distribution of silicon atoms was found to be as follows: at 250°C , 15.4% are T^0 species, 83.5% T^1 species, and 1.1% T^2 . At 350°C , it was found that 14.7% are T^0 species, 73.1% are T^1 , and 12.2% are T^2 . This shows that at higher temperature the methoxysilyl side groups react and cross-link.

Figure 5 shows the ^{29}Si NMR results for a mixture of 30:70 wt % TMSNB with MSQ. The spectra for the mixture after the (a) 250°C and (b) 350°C cure processes are presented. Three peaks at -44 , -58 , and -65 ppm were observed corresponding to the T^1 peak of the TMSNB, and the T^2 and T^3 peaks of the MSQ, respectively (according to the chemical shifts in the spectra of the individual components). A deconvolution process was necessary to properly resolve the area of the T^1 and T^2 peaks. Figure 6 shows the results of the deconvolution of the spectra. The plot shows that the concentration of T^1 species (far left) is reduced from 22 to 16% with an increase in cure temperature from 250 to 350°C , whereas the T^3 concentration (plotted at the far right of Fig. 6) increases from 53%

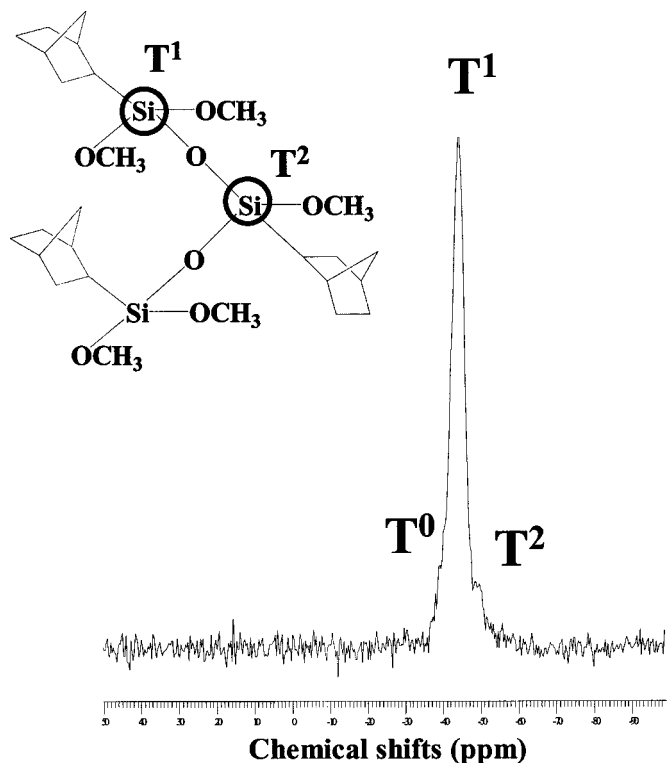


Figure 4. Molecular structure of TMSN and the ^{29}Si NMR spectrum after cure at 350°C for 1 h.

at 250°C to 62% at 350°C . The middle section of the plot in Fig. 6 shows the breakdown of the T^2 peak into three separate peaks at -50 , -56 , and -58 ppm corresponding to three different silicon T^2 environments. The -56 and -58 ppm peaks showed the highest concentration after the cure process at 350°C at 8 and 13% silicon atoms, respectively. Comparing these chemical shifts with those observed for the individual components, the T^2 peak at -50 ppm corresponds to T^2 species in TMSN and the peak at -58 ppm to those in MSQ. However, the peak at -56 ppm corresponds to a new silicon T^2 environment, only present in the TMSN:MSQ mixtures. This observation suggests that this third, new T^2 environment is the result of a chemical linkage between the MSQ and TMSN components in the mixture.

Similar NMR studies were conducted with the TESNB sacrificial polymer. The pure TESNB spectra after heat-treatment at 350°C shows the following distribution of silicon atoms: T^0 (-46 ppm) species at 21.4%, T^1 (-48 ppm) $[\text{NB-Si}\cdot(\text{OSi})(\text{OCH}_2\text{CH}_3)_2]$ at 74.6%, and T^2 (-53 ppm) $[\text{NB-Si}\cdot(\text{OSi})_2\text{OCH}_2\text{CH}_3]$ at 4% concentration.^{11,13} Compared to the TMSN, the TESNB polymer shows a higher concentration of silicon nuclei still in the T^0 form and less in the T^2 type. This is reasonable because the triethoxysilyl side group is less reactive than the trimethoxysilyl side group.¹⁵ For T^0 type species to convert into T^1 and T^2 nuclei, they need to undergo a hydrolysis and a condensation reaction creating the Si-O-Si bonds.

The ^{29}Si NMR results for a 30:70 wt % TESNB:MSQ mixture after heating to 350°C also show three peaks corresponding to the T^1 , T^2 , and T^3 species, analogous to the TMSN mixture. However, contrary to the T^2 deconvolution results for the TMSN mixture, only two T^2 peaks were observed for the TESNB:MSQ sample. The concentration distribution was found to be: 13% T^1 (-48 ppm), 18.3% T^2 species [10.2% (-56 ppm), and 8.1% (-58 ppm)], and 68.7% T^3 (-65 ppm). A 10 wt % TESNB sample also showed two T^2 peaks at -56 and -58 ppm even though it was cured at a lower

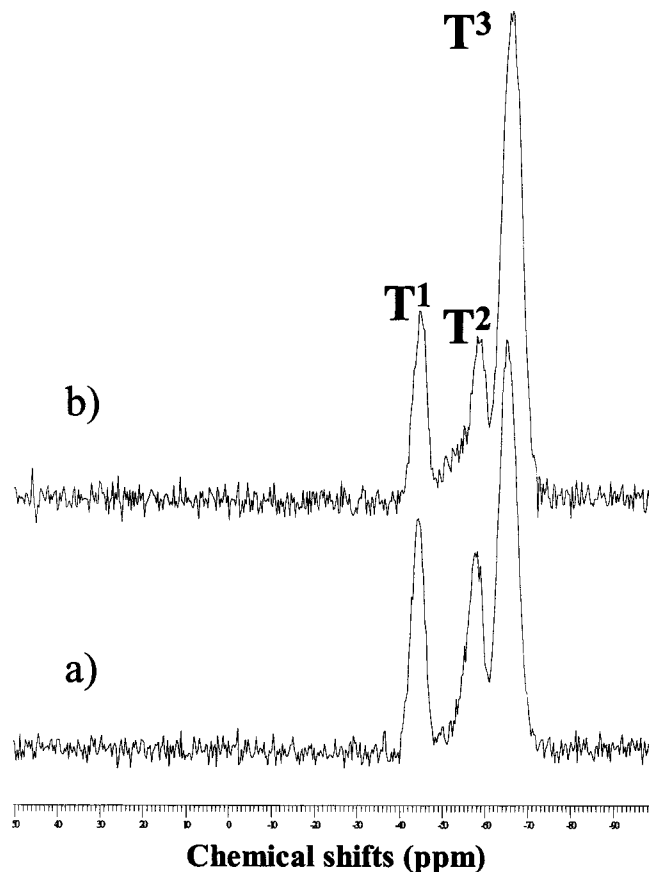


Figure 5. ^{29}Si NMR spectra for a mixture of 30:70 wt % TMSN:MSQ after cure at (a) 250°C for 30 min and (b) 350°C for 1 h.

temperature (250°C). Comparing the NMR results for the individual components (TESNB and MSQ), it appears that the T^2 peaks in the blends show only the peaks from the individual components: TESNB T^2 peak (~ -53 ppm), and the MSQ T^2 peak (-58 ppm). The absence of the third T^2 peak shows that the TESNB polymer does not bond to the MSQ in the sample.

The effect of adding an acid to the TESNB:MSQ mixtures was also investigated using ^{29}Si NMR. The results for the individual components and the mixtures after heat-treatment at 250°C show significant differences as compared to the samples without the acid.

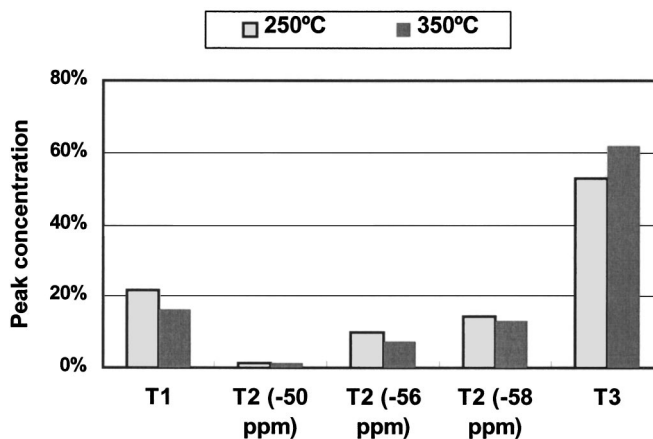


Figure 6. Deconvolution results for the ^{29}Si NMR spectra of a 30:70 wt % mixture of TMSN and MSQ.

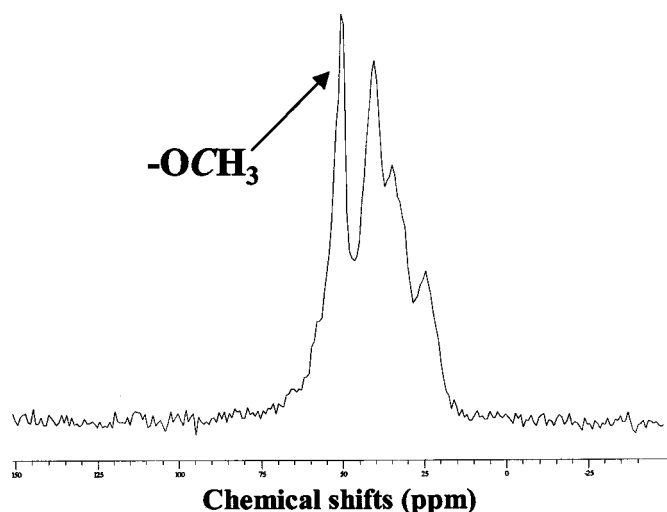


Figure 7. Solid-state ^{13}C NMR spectrum for TMSNB after cure process at 250°C for 30 min. Data collected with 1 ms contact time.

The T^2 and T^3 peaks of the MSQ have the same chemical shifts (-58 and -65 ppm, respectively), but the concentration of T^3 species increased to 94.4% in the case with the PAG (as opposed to the previously stated 71% without it), thus showing the catalytic effect of the acid in the condensation reaction of MSQ. Similarly, the acid catalyzed the hydrolysis and condensation reactions of TESNB. For the TESNB sample with PAG, the concentration distribution was found to be: 28.8% T^1 (-48 ppm), 53.2% T^2 (-56 ppm), and the new peaks of 4.2% T^3 (-66 ppm), 4.6% Q^2 (-90 ppm) $[(\text{CH}_3\text{CH}_2\text{O})_2\text{Si}(\text{OSi})_2]$, and 9.2% Q^3 species (-95 ppm) $[\text{CH}_3\text{CH}_2\text{OSi}(\text{OSi})_3]$.¹⁴ The appearance of Q-type silicon environments shows that the acid was of sufficient strength to break NB-Si bonds in the TESNB. Finally, a 10:90 wt % TESNB:MSQ mixture showed similar results regardless of the acid system used to prepare the sample. The silicon distributions for these were found to be, with PAG, 11.8% (-54 ppm), 0.6% (-56 ppm), and 7.8% (-58 ppm) T^2 species, and 79.8% T^3 species (-65 ppm); and with HCl, 10.5% (-54 ppm), 2.2% (-56 ppm), and 7.1% (-58 ppm) T^2 species, and 80.2% T^3 species (-65 ppm). The peaks at -56 and -58 ppm correspond to the T^2 species in TESNB and MSQ, respectively. The third T^2 environment (-54 ppm), characteristic only of TESNB mixtures with added acid catalyst, suggests that a chemical bond was created between the TESNB polymer and the MSQ in this case, analogous to the TMSNB mixtures.

Solid-state ^{13}C NMR.—Solid-state ^{13}C NMR experiments were conducted to investigate the reactivity of the methoxysilyl and ethoxysilyl side groups as a function of cure temperature for both the pure TMSNB and TESNB sacrificial polymers, as well as the NB:MSQ mixtures. Figure 7 shows the ^{13}C NMR spectrum for TMSNB after curing at 250°C for 30 min. Four major peaks are observed at 50, 40, 34.4, and 25 ppm (downfield from TMS). The three peaks at 25, 34.4, and 40 ppm correspond to carbon atoms within the norbornene ring. The largest peak, at 50 ppm, is a combination of the signal from the methoxy groups present in the molecules, which usually have a chemical shift around 55 ppm,¹⁶ and another norbornene peak. The change in the concentration of methoxy groups ($-\text{OCH}_3$) with temperature was monitored through the variation in the integral of this peak as shown in Fig. 8. To avoid differences induced from variations in the mobility of the species (cross polarization techniques enhance signals based on mobility), the ratio of the methoxy to each of the three norbornene peaks (at 25, 34.4, and 40 ppm) was used. The norbornene peaks were used as a reference for calculating the ratios because in the reaction se-

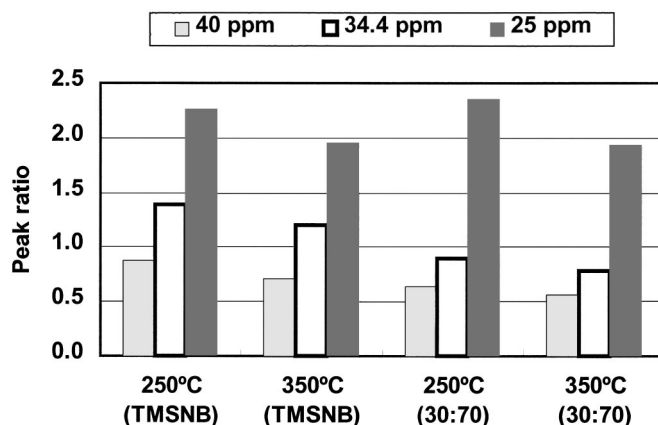


Figure 8. Plot of the variations in the methoxy groups as a function of temperature for a TMSNB sample (left), and a 30:70 wt % mixture of TMSNB with MSQ (right).

quence, these peaks remain unchanged (at least within this temperature range). Only the methoxy groups react in a hydrolysis and condensation process to form Si—O—Si bonds between polymer chains. Figure 8 shows the ratios as a function of temperature for two different samples. The results for a pure TMSNB sample are shown on the left side of Fig. 8 and the 30:70 wt % TMSNB:MSQ mixture is shown on the right side. In both cases, increasing the cure temperature from 250 to 350°C causes a reduction of all the ratios, due to a reduction in the methoxy group concentration. For the TMSNB sample, an average 17.5% reduction in the methoxy concentration is observed within this temperature range. This reduction is due to the hydrolysis and condensation reaction. However, there still remains a methoxy population even after heat-treatment at 350°C . This is confirmed in the ^{29}Si NMR spectra. The highest stage that the polymer achieves at 350°C is a T^2 form. On average, one of the three original methoxy groups in TMSNB remains unreacted. Methoxy groups are also still represented in the T^1 and T^0 silicon environments.

The ^{13}C NMR spectrum for TESNB is shown in Fig. 9. In this polymer, the norbornene peaks occur at the same chemical shifts previously stated for the TMSNB polymer, at 51, 40, 34.4, and 26 ppm. The two end peaks correspond to unreacted ethoxy groups ($-\text{OCH}_2\text{CH}_3$) in the sample. The carbons in the methylene group

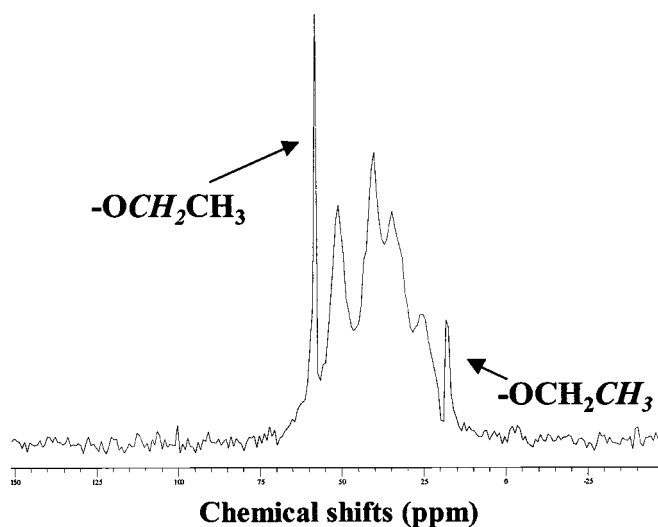


Figure 9. ^{13}C NMR spectrum for TESNB after cure at 250°C . Contact time: 1 ms.

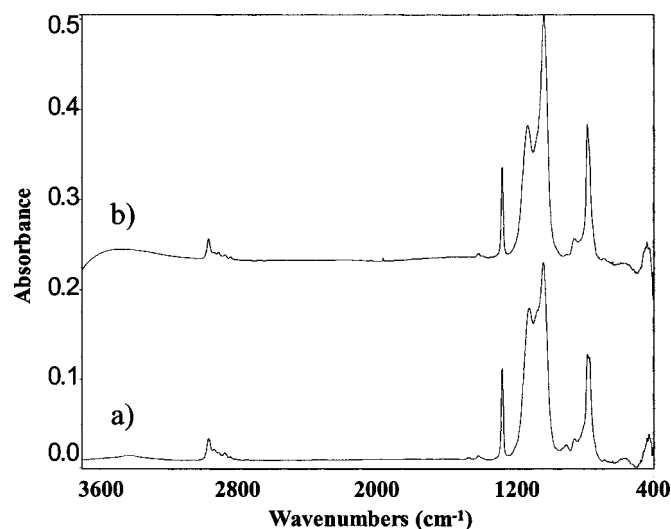


Figure 10. FTIR spectra for MSQ (a) before cure and (b) after cure at 425°C for 1.5 h.

(—CH₂—) show a chemical shift of 58 ppm from TMS (NMR reference), and the methyl groups (—CH₃) show a shift at 18 ppm.^{13,16} A study of the evolution of the ethoxy groups in this sacrificial polymer system as a function of cure temperature was performed. The results show little variation in the concentration of the groups between 250 and 350°C indicating minimal reactivity of these moieties within this temperature range. These results are consistent with the ²⁹Si NMR where there was limited reaction of the ethoxy groups compared with TMSNB.

Fourier transform infrared spectroscopy (FTIR).—Infrared spectroscopy was used to follow the MSQ cure process. The changes in the silanol and the siloxane concentrations were monitored. The FTIR spectra for MSQ before and after cure are shown in Fig. 10. Spectrum 10a is for MSQ after spin-coating and baking in a nitrogen atmosphere at 180°C for 10 min, and spectrum 10b is after furnace curing the MSQ sample at 425°C for 1.5 h. Silanol (Si—OH) vibrations occur in the 3400 to 3500 cm⁻¹ range, as can be seen in Fig. 10a (the spectrum before cure) with the broad peak centered at 3427 cm⁻¹. A change in the peak ratio was measured from 0.066 at 180°C to 0.0 in the spectrum after cure at 425°C for 1.5 h (peak ratios taken with respect to an internal reference in MSQ). The peak height reduced with cure temperature due to the condensation reaction, which depletes the silanol moieties in MSQ to create Si—O—Si linkages. The asymmetric and symmetric CH₃ stretches at 2969 and 2876 cm⁻¹, respectively, were also followed. Although MSQ contains mostly methyl groups, other C—H peaks were observed in the region between 2843 and 2969 cm⁻¹. These C—H species were observed in the ¹³C NMR spectra for MSQ. It has been suggested that residues from the MSQ synthesis process are present in commercial MSQ resins.¹⁷ The dominant peaks in the MSQ spectra are

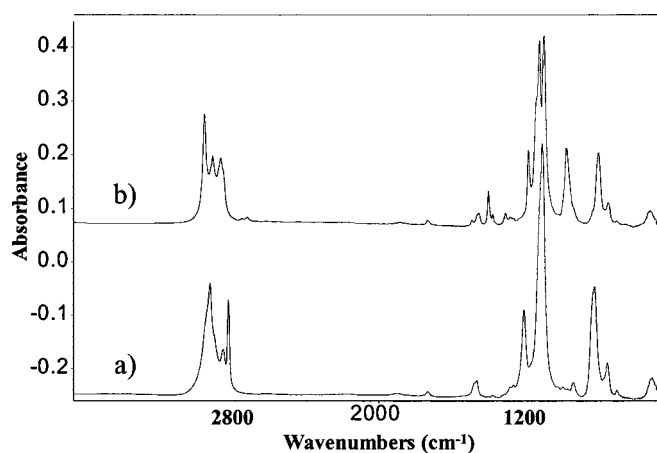


Figure 11. FTIR spectra for a (a) TMSNB and a (b) TESNB film before cure (after 180°C treatment for 10 min).

the Si—CH₃ symmetric stretch at 1271 cm⁻¹, the siloxane bonds (Si—O—Si) for silsesquioxanes at 1114 and 1033 cm⁻¹ (1123 and 1030 cm⁻¹, respectively, after cure), and the O—Si—CH₃ vibrations at 855 and 779 cm⁻¹.¹⁸⁻²⁰

Table I shows the peak ratios for five MSQ FTIR peaks as a function of cure temperature. In this case, the symmetric Si—CH₃ peak at 1271 cm⁻¹ was used as the reference because ²⁹Si NMR studies have shown that this bond is stable at high temperatures. No Q-type peaks were observed, which shows that the Si atoms retained their —CH₃ bonds. Therefore, the peak heights at 2969, 1114, 1033, 855, and 779 cm⁻¹ were measured with respect to this internal reference. In Table I, the ratio of the peaks at 1033 cm⁻¹ (for long O—Si—O chains) increase at the expense of the other siloxane peak at 1114 cm⁻¹ (for short O—Si—O chains). That is, the first peak increased by 27% whereas the second one was 16% lower. These peak changes are characteristic of the transition of MSQ into a three-dimensional network.¹⁸ Also presented in Table I are the peak ratios for the O—Si—CH₃ bonds at 855 and 779 cm⁻¹, which show little variation as a function of temperature. This provides another indication of the stability of the Si—CH₃ bonds.

The FTIR spectra for TMSNB and TESNB films before cure (after 180°C treatment for 10 min) are shown in Fig. 11a and b, respectively. The main peaks in the spectra are the asymmetric and symmetric CH₃ stretches, which for TMSNB occur at 2942 and 2868 cm⁻¹, and for TESNB at 2972 and 2882 cm⁻¹, respectively. The Si—OCH₃ stretching vibration in TMSNB is at 2839 cm⁻¹, the CH₂ asymmetric stretch in TESNB is at 2927 cm⁻¹, and the CH₃ asymmetric bending deformations are at 1454 cm⁻¹ in TMSNB and at 1442 cm⁻¹ in TESNB. Also relevant in the TMSNB spectrum are the CH₃ rocking vibration (from Si—OCH₃) at 1191 cm⁻¹, the Si—O—C asymmetric stretch at 1089 cm⁻¹, and the Si—C stretch at 797 cm⁻¹. Similarly in the TESNB spectrum, the Si—OCH₂CH₃

Table I. FTIR peak ratios for MSQ and a 30:70 wt % TMSNB:MSQ film as a function of the cure temperature.

Peak wavenumber (cm ⁻¹)	Peak ratios				
	2969	1114	1033	855	779
Thermal history for MSQ					
Baked at 180°C		1.774	2.124	0.234	1.139
Cured at 250°C/30 min		1.586	2.431	0.241	1.353
Cured at 350°C/30 min		1.496	2.639	0.218	1.479
Cured at 425°C/1.5 h	0.208	1.495	2.703	0.248	1.505
Thermal history for 30:70 wt % TMSNB:MSQ					
Cured at 425°C/1.5 h	0.186	1.473	2.626	0.220	1.297

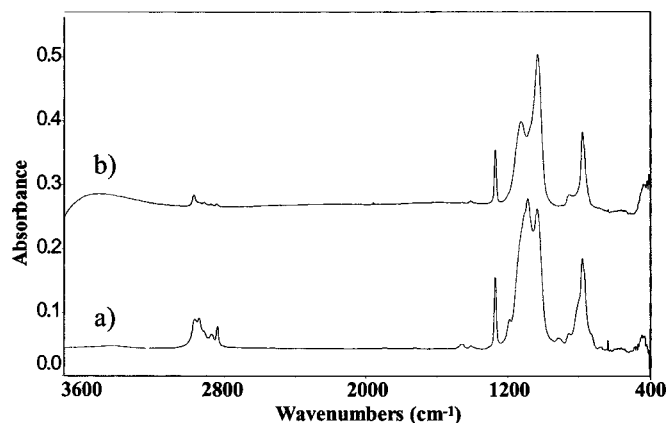


Figure 12. FTIR spectra for a 30:70 wt % TMSNB:MSQ mixture film (a) before cure and (b) after cure at 425°C for 1.5 h.

vibration at 1166 cm^{-1} , the strong doublet for Si—O—C asymmetric stretches of the ethoxysilane groups at 1105 and 1080 cm^{-1} , the Si—O—C symmetric stretch at 953 cm^{-1} , and the Si—C stretch at 776 cm^{-1} can be seen. The FTIR spectra as a function of cure temperature have been collected for the sacrificial polymer systems. Little change was observed in the peaks with increasing cure temperature in the range from 180 to 350°C. (Note: all spectra were collected at room temperature after curing.) The FTIR spectra for these films were compared to ones after a furnace cure at 425°C for 1.5 h, where the polymers decomposed (this process simulates the one used to create porosity in the films). The spectra confirmed that heating the TMSNB or TESNB polymers results in nearly complete decomposition and removal of the sacrificial polymer. In both cases, however, a small absorption peak at approximately 1100 cm^{-1} was observed, which indicates that a small amount of silicon oxide residue remained after decomposition. Comparing the absorption in the siloxane region before and after treatment at 425°C showed that $\sim 11\%$ of the TMSNB and 7% of the TESNB remained as residue.

FTIR spectroscopy was also used to monitor the presence of the sacrificial polymer within the TMSNB:MSQ and TESNB:MSQ films. These studies were conducted as a function of temperature. Figure 12 shows the spectra for a 30:70 wt % mixture of TMSNB in MSQ before and after cure. In Fig. 12a before curing, both components can be identified. After curing at 425°C (Fig. 12b), the spectrum is essentially the same as cured MSQ, Fig. 10b. The peak ratios for MSQ with and without TMSNB were calculated with reference to the Si—C peak, and are presented at the bottom of Table I. The peak ratios for MSQ with and without the sacrificial polymer are the same, within experimental error, which shows that the decomposition products of the TMSNB polymer permeated through the MSQ matrix to leave an almost pure MSQ film behind. Similar results were also observed for the TESNB:MSQ mixtures after decomposition of the sacrificial polymer within the films.

Thermogravimetric analysis (TGA).—Thermogravimetric studies were conducted with the TMSNB and TESNB polymers in order to characterize their performance as sacrificial materials. Figure 13 shows the decomposition curve for both polymers as a function of temperature and time. The two curves show the same decomposition profile. The TMSNB shows an initial 5% weight loss at 121°C that was most likely due to residual solvent. The boiling point of the MIBK solvent is 118°C. After normalizing the curve for the solvent removed, the TMSNB and TESNB polymers show a 5% wt loss at 357°C, and a 10% wt loss at 375°C. The onset of decomposition for both polymers occurred at approximately 380°C followed by a sharp drop in weight. The estimated weight loss for both polymers was calculated based on the ^{29}Si NMR results. In both cases, the expected weight loss at 350°C was determined from the concentration

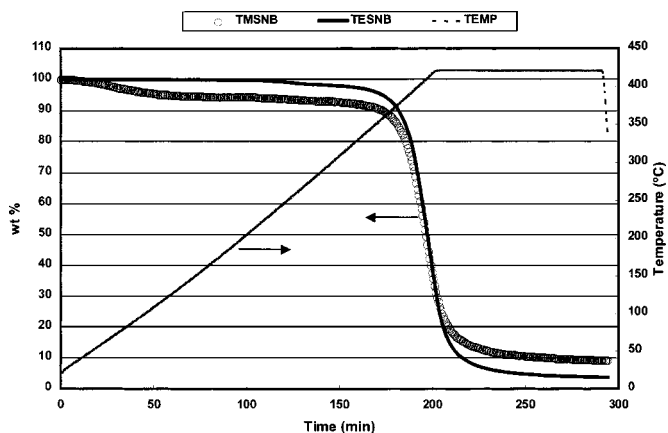


Figure 13. Weight loss as a function of time and temperature for the TMSNB and TESNB sacrificial polymers.

of silicon atoms at the different reacted and unreacted stages (T^0 to T^2 species), or from the degree of conversion of the methoxysilyl and ethoxysilyl groups in the hydrolysis and condensation reactions. The estimated weight loss for TMSNB at 350°C was 6.8%, and 9.2% for TESNB. Thus, the 5 and 10% wt losses observed for both polymers in the TGA at 357 and 375°C, respectively, agree well with the estimated values. The small discrepancies can be attributed to the difference between the dynamic data obtained in the TGA and the ^{29}Si NMR results obtained after a cure process at 350°C for 1 h. The TMSNB sample shows a final residue of 9.6 wt %, while the TESNB polymer has only 3.7 wt % residue.

TESNB samples with different weight-average molecular weights ($M_w \sim 39,000$ -180,000) have been investigated. The TGA shows that the residue in each case was from 2 to 5 wt % after decomposition at 425°C. The IR absorbance of the residue for the TMSNB and TESNB polymers was previously shown in the FTIR spectra after decomposition at high temperature. The decomposition products are important because they will contribute to the dielectric constant. The amount of residue observed in the TGA results agreed with the values estimated from the FTIR spectra for the materials. For TMSNB, a 9.6 wt % residue was observed in the TGA results, whereas an 11 wt % was estimated from the FTIR spectrum after heating at 425°C for 1.5 h. Similarly for TESNB, a 3.7 wt % residue was measured in the TGA, and a 7 wt % was estimated from the FTIR spectrum. The differences are within the experimental error.

The TGA curves for 30:70 wt % mixtures of TMSNB:MSQ and TESNB:MSQ are shown in Fig. 14. A weight loss of about 6% was

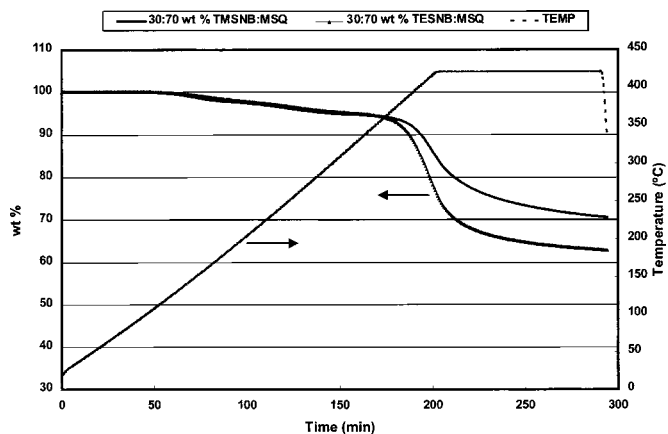


Figure 14. Weight loss from the 30:70 wt % mixtures of TMSNB and TESNB with MSQ as a function of time and temperature.

observed with both samples in the range from 128 to 393°C for TMSNB, and from 125 to 379°C for TESNB. This is similar to the pure MSQ sample where a 12% wt loss was observed between 138 and 333°C due to the creation of Si—O—Si linkages through the condensation reaction of the silanol groups (less than 2% wt loss was observed at 425°C). In comparison, the estimated weight loss from the evolution of water in MSQ, based on the assumption that each monomer unit contains four CH₃SiO groups and four hydroxyl (OH) groups (determined from the known chemical structure of the final product, and the ratio of CH₃ to OH groups observed from IR as compared to the ratio of the same groups in the spectrum for methyl alcohol), was calculated to be 11.7%. This corresponds to 0.5 water molecules generated per silicon atom in the structure of MSQ.

The onset of degradation of the TESNB in the 30:70 wt % mixture with MSQ occurs at about 380°C (Fig. 14), the same as observed with the pure polymer sample. Thus, the TESNB decomposition and weight loss does not seem to be affected by the presence of the MSQ in the sample. With TMSNB, the weight loss starts at a higher temperature (~393°C) in contrast to the polymer itself. The total weight loss observed for the 30:70 wt % TMSNB:MSQ mixture was 29.5 wt %, and for the TESNB:MSQ sample was 37 wt %. For comparison, the estimated weight losses for the sacrificial polymer:MSQ mixtures were calculated from the measured weight losses of the individual components and their ratio in the mixtures (30:70 wt %). The estimated weight loss was 36 wt % for the TMSNB:MSQ mixture, and 38 wt % for the TESNB:MSQ mixture. Therefore, the experimental and estimated values for the TESNB:MSQ mixture agree very well, but the measured weight loss for the TMSNB:MSQ sample (29.5 wt %) was slightly lower than expected (36 wt %).

Discussion

The critical difference between TMSNB and TESNB as sacrificial materials for the development of porous dielectrics is the resulting pore microstructure created after decomposition of the polymer within the MSQ matrix. In the case of TMSNB, nanosize pores were created within the films, whereas in the TESNB samples, only large pores at the surface were observed after heating to 425°C. These differences have been attributed to the chemical interaction between the components in the mixture. In order to achieve a highly porous film with nanometer-size pore distribution, a chemical bond between the porogen (sacrificial) material and the MSQ is required. Failure to enhance the chemical bonding of the components results in phase-separation of the porogen from the matrix, and eventually leads to the creation of large pores.

TMSNB and TESNB sacrificial polymers.—From the TGA data in Fig. 13, it is clear that both polymers, TMSNB and TESNB, have a low weight loss region (<10 wt %) below 380°C and a high weight loss region between 380°C and the final cure temperature of 425°C. To our understanding, the polymer weight loss in each temperature regime is controlled by a different mechanism. At temperatures below 380°C, most of the weight loss occurred due to the cross-linking reactions of the polymer side groups, which involve the removal of water and alcohols through the hydrolysis and condensation of the alkoxysilyl groups. The reaction scheme was previously presented in Eq. 1 to 3. The hydrolysis of the alkoxysilyl groups is the rate-limiting step and involves the nucleophilic attack of the silicon atom by the OH group in water (in this case, moisture from the environment or residual moisture in the solvent system).²¹ The condensation reaction takes place almost simultaneously with hydrolysis and therefore, the analytic detection of intermediate silanol groups is not feasible.¹⁷ These reactions convert the alkoxysilyl groups into Si—O—Si linkages, which are responsible for branching and cross-linking the polymer chains. As the hydrolysis and condensation reactions proceed, there is a sequential conversion of T⁰ (unreacted alkoxy groups) to T¹ species (one Si—O—Si linkage formed), and from T¹ to T² species (two Si—O—Si linkages). This conversion is evident from the comparison of the T⁰, T¹, and T²

peak concentrations at 250 and 350°C for the TMSNB and TESNB polymers (as determined from the ²⁹Si NMR experiments). Therefore, the higher the concentration of T¹ and T² silicon environments observed in the polymers, the larger the extent of branching (T¹) and cross-linking (T²) developed between the chains. Since the methoxysilyl side groups are more reactive (undergo hydrolysis more easily) than the ethoxysilyl groups,^{15,22} the extent of cross-linking of the TMSNB polymer should be higher, as compared to the TESNB polymer, at any given temperature. This hypothesis is confirmed by the ²⁹Si NMR results, which showed a higher concentration of T² species in TMSNB (~12%) as compared to TESNB (~4%) after heat-treatment at 350°C for 1 h. At this temperature, a significantly higher concentration of unreacted (T⁰) triethoxysilyl groups was also observed as compared to trimethoxysilyl side groups. Furthermore, these observations are also consistent with the ¹³C NMR analysis of the TMSNB (Fig. 8) and TESNB polymers, which showed a higher reduction in the methoxy group concentration between 250 and 350°C as compared to the change in the ethoxy group concentration. The lower concentration of T² silicon atoms in TESNB, or the lower reactivity of the TESNB polymer, could be attributed to the steric hindrance of the relatively large ethoxy groups as compared to the methoxy groups, which could inhibit further reaction of the T¹ species. In this regard, it must be noted that no T³ species were observed in the TESNB or the TMSNB by ²⁹Si NMR analysis, which suggests that the reaction of the third alkoxy group was severely hindered in both cases.

In the temperature regime greater than 380°C, the polynorbornene degradation has been shown to occur.²³ Although the degradation mechanisms are difficult to specify, they can have two competing pathways²⁴ that involve (i) polymer chain scission and (ii) cross-linking reactions of the alkoxysilyl side groups, which tend to stabilize and increase the thermal stability of the polymer. The degradation of polynorbornene has been found to occur by chain scission through a combination of depropagation and transfer reactions.²⁵ The presence of cross-links hinders the volatilization of the polymer, and the subsequent cleavage of the norbornene rings from the cross-linked Si—O—Si groups can result in residue due to the higher thermal stability of these groups. Previous decomposition studies performed with a 90:10 (molar %) BuNB:TESNB copolymer showed residues of ~1.4 to 1.9 wt %, ²⁵ whereas a 3.7 wt % residue was observed for the TESNB polymer in this study (under similar heat-treatment). The higher residue can be attributed to the fact that the sacrificial polymers used in this study were homopolymers with triethoxysilyl groups in every repeat unit, as opposed to the previous copolymer in which only one in ten units had a triethoxysilyl moiety. The higher concentration of triethoxysilyl groups can give rise to a higher degree of cross-linking and hence, a higher residue. It is important to note that the extent of cross-linking that occurs below 380°C (onset of degradation) can have a significant impact on the degradation rate and on the final wt % residue obtained after heat-treatment at 425°C. Since the TMSNB polymer showed a higher extent of cross-linking as compared to the TESNB polymer (as indicated above), it is bound to have a higher thermal stability and therefore, would be expected to yield a higher residue than the TESNB polymer. Indeed, the TGA studies showed a 9.6 wt % residue for TMSNB compared to only 3.7 wt % residue for TESNB after treatment at 425°C for 1.5 h.

TMSNB:MSQ and TESNB:MSQ mixtures.—As stated previously, the MSQ resins in solution contained silanol groups that condense upon heating to high temperature. In the absence of additional water or an external catalyst, the alkoxysilyl groups also rely on high temperature to increase the rate of the hydrolysis and condensation reactions, but at any given temperature the methoxysilyl moieties are more reactive than the ethoxysilyl groups. Furthermore, the higher reactivity of the methoxy groups, as compared to ethoxy groups, with hydroxy (—OH) functional polymers has also been demonstrated.²² The combination of a higher extent of hydrolysis,

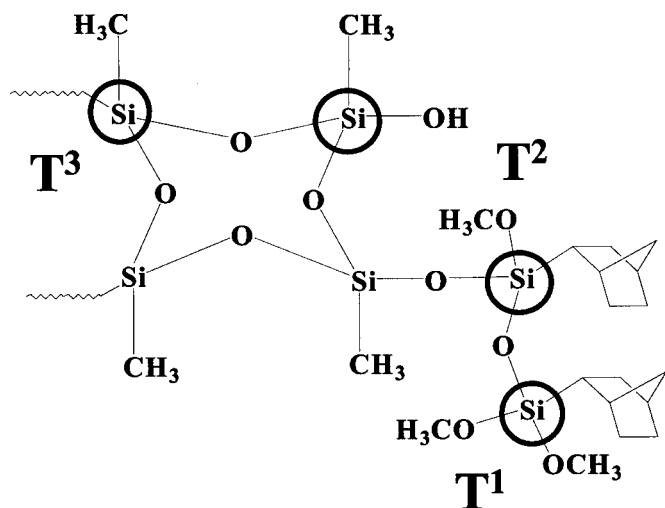


Figure 15. Chemical structure showing the chemical bond between the TMSNB polymer and the MSQ matrix as determined from ^{29}Si NMR.

and a higher reactivity with the silanol groups in MSQ (Eq. 2), therefore, enhances the miscibility of the TMSNB with the MSQ. The formation of silanol groups in the TMSNB not only enhances the solubility with MSQ due to potential hydrogen bonding between the —OH groups, but also expands the reaction pathways by which the TMSNB can bond with the MSQ matrix (Eq. 3). The hypothesis of potential chemical bonding between the TMSNB and the MSQ has been corroborated with the detection of a new T^2 silicon environment (-56 ppm) in the ^{29}Si NMR spectra for the TMSNB:MSQ mixtures (Fig. 6). Figure 15 shows a schematic of the chemical structure formed from the condensation reactions between the TMSNB and the MSQ, as suggested by the T^2 -type species detected in the NMR analysis; this implies that two of the methoxysilyl groups must have reacted to form Si—O—Si linkages. Furthermore, TEM micrographs (Fig. 1) have shown pores of approximately the same size (~ 3 to 10 nm) within the bulk of the films regardless of the concentration of sacrificial TMSNB used to prepare the samples. For comparison, the pores formed from the decomposition of a single polymer molecule would have a diameter of 3 nm, assuming spherical geometry, density of 1 g/cm^3 , and molecular weight of $57,000$. Thus, the pores in the films using TMSNB as the sacrificial material were approximately the same as the size of the single polymer molecules. These observations show that there was excellent miscibility between the two components of the mixture (microscopic distribution). Finally, the TGA results for the TMSNB:MSQ system are also consistent with these observations (Fig. 13 and 14). As stated previously, cross-linking of the polymer chains has the effect of imparting higher thermal stability to the polymer. In the case of the mixtures, the chemical bonds between the TMSNB and the MSQ improved the thermal stability of the TMSNB. The onset of degradation of the polymer occurred at a higher temperature, and a slightly higher residue (~ 6 wt %) was observed as compared to the pure polymer samples.

Due to the lower reactivity of the ethoxysilyl groups, and the steric hindrance of the relatively large ethoxy groups, the TESNB is expected to be less miscible in the MSQ compared to TMSNB. The lower miscibility of the two components and lower reactivity of TESNB caused phase separation in the mixtures. This was corroborated with a series of TEM and AFM studies performed on the TESNB:MSQ films after heat-treatment at 425°C . The TESNB:MSQ films did not show porosity within the bulk of the films, and the surface topography studies showed the development of large cavities at the surface upon exposure of the films to the decomposition temperature of the TESNB (Fig. 2). The AFM observations indicated that the TESNB polymer phase separated and sub-

sequently dewetted from the MSQ material underneath. This dewetting phenomenon has been observed previously by Muller *et al.*²⁶ ^{29}Si NMR analysis of the TESNB:MSQ mixtures did not show the occurrence of the new T^2 peak which was characteristic of a chemical bond between the TMSNB and the MSQ. The onset of degradation of the polymer within the mixture (TESNB:MSQ) occurred at the same temperature as the pure polymer, and the measured weight loss for the mixture matched exactly the estimated weight loss for each component. Therefore, these results further confirm the phase separation of the TESNB from the MSQ matrix.

Finally, it is important to note that the differences in the pore microstructure developed from the TMSNB:MSQ and the TESNB:MSQ blends were influenced by the initial miscibility of the components in the mixture. That is, the combination of a higher solubility and higher reactivity between the TMSNB and the MSQ were responsible for the TMSNB remaining dispersed within the MSQ matrix. On the contrary, poor miscibility between the TESNB and the MSQ induced the immediate phase-segregation of the components upon spin coating. In this case, the delayed hydrolysis of the TESNB polymer was responsible for the lack of miscibility with MSQ. This hypothesis was further corroborated with the use of an acid catalyst in the TESNB:MSQ mixture, which enhanced the dispersion of the TESNB in MSQ. The ^{29}Si NMR analysis showed the new T^2 environment (-54 ppm), which was analogous to the TMSNB:MSQ mixtures. The analysis showed a reduction in the surface roughness and pore size of the TESNB:MSQ films with PAG as compared to the films without the acid.

Conclusions

Studies on the chemical structure of the MSQ-sacrificial polymer mixtures have demonstrated that variations in the pendant group attached to the norbornene backbone can cause significant differences in the resulting microstructure of the porous films. In one case, the use of TMS moieties resulted in porous films with pores of ~ 3 to 10 nm in diameter. ^{29}Si NMR studies performed with the mixtures identified a chemical bond between the MSQ matrix and the sacrificial material prior to decomposition of the polymer and creation of the pores. On the other hand, TES functional groups were not observed to form a chemical linkage between the polymer and the MSQ matrix, and therefore, the sacrificial material phase-separated from the inorganic matrix. In these samples, surface topography studies were used to identify cavities on the order of ~ 300 nm in diameter that corresponded to the decomposition sites of the segregated sacrificial polymer (TESNB) on top of an MSQ layer. Improvements in the surface roughness and the porosity of the TESNB:MSQ films were observed upon addition of an acid catalyst to the TESNB:MSQ mixture. ^{29}Si NMR results showed no bonding of the TESNB to the MSQ, except when an acid was added to the TESNB:MSQ mixture.

Acknowledgments

The contribution of Barbara Tsuie for synthesizing the TMSNB and TESNB sacrificial polymers used in this study is gratefully acknowledged. The authors acknowledge Johannes Leisen (School of Textile and Fiber Engineering, Georgia Institute of Technology) and Leslie Gelbaum (NMR Center, Georgia Institute of Technology) for their assistance with the NMR experiments and helpful discussions on the topic. The contribution of Dr. James Conner (Motorola, Austin) for the TEM analysis is also gratefully acknowledged.

Georgia Institute of Technology assisted in meeting the publication costs of this article.

References

1. A. M. Padovani, L. Rhodes, L. Riester, G. Lohman, B. Tsuie, J. Conner, S. A. Bidstrup Allen, and P. A. Kohl, *Electrochem. Solid-State Lett.*, **4**, F25 (2001).
2. L. Peters, *Semicond. Int.*, **23**, 108 (2000).
3. J. H. Golden, C. J. Hawker, and P. S. Ho, *Semicond. Int.*, **24**, 79 (2001).
4. C. T. Chua, G. Sarkar, and X. Hu, *J. Electrochem. Soc.*, **145**, 4007 (1998).

5. N. P. Hacker, G. Davis, L. Figge, T. Krajewski, S. Lefferts, J. Nedbal, and R. Spear, *Mater. Res. Soc. Symp. Proc.*, **476**, 25 (1997).
6. P. Eaton, P. Holmes, and J. Yarwood, *J. Appl. Polym. Sci.*, **82**, 2016 (2001).
7. D. A. Skoog, F. J. Holler, and T. A. Nieman, *Principles of Instrumental Analysis*, 5th ed., Saunders College Publishing, Philadelphia, PA (1998).
8. C. Dybowski and R. L. Lichter, *NMR Spectroscopy Techniques*, Marcel Dekker, Inc., New York (1987).
9. C. Nguyen, C. J. Hawker, R. D. Miller, E. Huang, and J. L. Hedrick, *Macromolecules*, **33**, 4281 (2000).
10. J. F. Remenar, C. J. Hawker, J. L. Hedrick, S. M. Kim, R. D. Miller, C. Nguyen, M. Trollsas, and D. Y. Yoon, *Mater. Res. Soc. Symp. Proc.*, **511**, 69 (1998).
11. L. Bourget, D. Leclercq, and A. Vioux, *J. Sol-Gel Sci. Technol.*, **14**, 137 (1999).
12. R. Joseph, S. Zhang, and W. T. Ford, *Macromolecules*, **29**, 1305 (1996).
13. K. J. Shea, D. A. Loy, and O. Webster, *J. Am. Chem. Soc.*, **114**, 6700 (1992).
14. H. Jo and F. D. Blum, *Langmuir*, **15**, 2444 (1999).
15. V. Gualandris, F. Babonneau, M. T. Janicke, and B. F. Chmelka, *J. Sol-Gel Sci. Technol.*, **12**, 75 (1998).
16. W. W. Simons, *The Sadtler Guide to Carbon-13 NMR Spectra*, Sadtler, Philadelphia, PA (1983).
17. R. H. Baney, M. Itoh, A. Sakakibara, and T. Suzuki, *Chem. Rev.*, **95**, 1409 (1995).
18. C. Y. Wang, Z. X. Shen, and J. Z. Zheng, *Appl. Spectrosc.*, **54**, 209 (2000).
19. G. Socrates, *Infrared Characteristic Group Frequencies*, John Wiley & Sons, Inc. New York (1980).
20. D. L. Vien and N. B. Colthup, *The Handbook of Infrared and Raman Characteristic Frequencies of Organic Molecules*, Academic Press, Inc., New York (1991).
21. C. J. Brinker, *J. Non-Cryst. Solids*, **100**, 31 (1988).
22. G. L. Witucki, *J. Coat. Technol.*, **65**, 57 (1993).
23. D. Bhusari, H. A. Reed, M. Wedlake, A. M. Padovani, S. A. Bidstrup, and P. A. Kohl, *J. MEMS*, **10**, 400 (2001).
24. I. Banik, A. K. Bhowmick, S. V. Raghavan, A. B. Majali, and V. K. Tikku, *Polym. Degrad. Stab.*, **63**, 413 (1999).
25. M. D. Wedlake and P. A. Kohl, *J. Mater. Res.*, **17**, 632 (2002).
26. P. Muller-Buschbaum, J. S. Gutmann, and M. Stamm, *J. Macromol. Sci., Phys.*, **B38**, 577 (1999).